BIOCHEMISTRY
including biophysical chemistry & molecular biology

Rapid Report

pubs.acs.org/biochemistry

Chemically Induced Changes to Membrane Permeability in Living Cells Probed with Nonlinear Light Scattering

Michael J. Wilhelm,* Mohammad Sharifian Gh., and Hai-Lung Dai

Department of Chemistry, Temple University, 1901 North 13th Street, Philadelphia, Pennsylvania 19122, United States

Supporting Information

ABSTRACT: Second-harmonic light scattering (SHS) permits characterization of membrane-specific molecular transport in living cells. Herein, we demonstrate the use of time-resolved SHS for quantifying chemically induced enhancements in membrane permeability. As proof of concept, we examine the enhanced permeability of the cytoplasmic membrane in living *Escherichia coli* following addition of extracellular adenosine triphosphate (ATPe). The transport rate of the hydrophobic cation, malachite green, increases nearly an order of magnitude following addition of 0.1 mM ATPe. The absence of an ATPe-enhanced permeability in liposomes strongly suggests the induced effect is protein-mediated. The utility of SHS for elucidating the mechanism of action of antimicrobials is discussed.

Antimicrobial resistance is an ever-present worldwide threat that demands the continual identification of new and distinct viable classes of antibiotic drugs to quell the pandemic spread of microbial pathogens.[1,2] One successful strategy for inducing antimicrobial activity is to increase the permeability of the microbial membrane, thereby weakening the cell's first line of defense.[1,3,4] For example, a number of antimicrobial peptides are polycationic species and initially interact with cells by electrostatically binding to the anionic membrane surfaces.[3−8] Above a critical concentration, the surface-bound peptides begin constructing passive transport channels into the cell, thereby enhancing the membrane permeability.[3−8] While the potency of a potential antimicrobial candidate is easily tested (it either does or does not kill the cell), the surface-specific molecular-level interactions, which are necessary for understanding and subsequently optimizing the antimicrobial efficacy, are not as easily quantified. To address this, it is prudent to establish a protocol capable of surface-specific characterization of antimicrobial−membrane interactions.

Membrane-specific molecular transport can be characterized in real time using second-harmonic light scattering (SHS).[9−12] This approach is based on the nonlinear optical phenomenon second-harmonic generation (SHG), in which a fraction of a probe laser is scattered at twice the frequency of the original source by interacting with matter.[13] In general, molecules that lack inversion symmetry are capable of producing SHG. However, disordered ensembles of SHG-active molecules (e.g., molecules dissolved in a liquid colloidal suspension) produce no coherent SHG, as SH fields generated by isotropically oriented molecules cancel one another. Nevertheless, when SHG-active molecules align on the surface of a colloidal object (e.g., biological cell), the SH fields constructively interfere and generate a coherent SH response. SHS can be detected in real time, and the generated signal is proportional to the square of the molecular concentration on the surface of the colloidal object.[14−19]

As shown in Figure 1, SHS is capable of monitoring molecular transport across a membrane and is therefore sensitive to membrane permeability, by taking advantage of the opposite orientations of the opposing leaflets in a membrane bilayer. Specifically, as SHG-active molecules adsorb

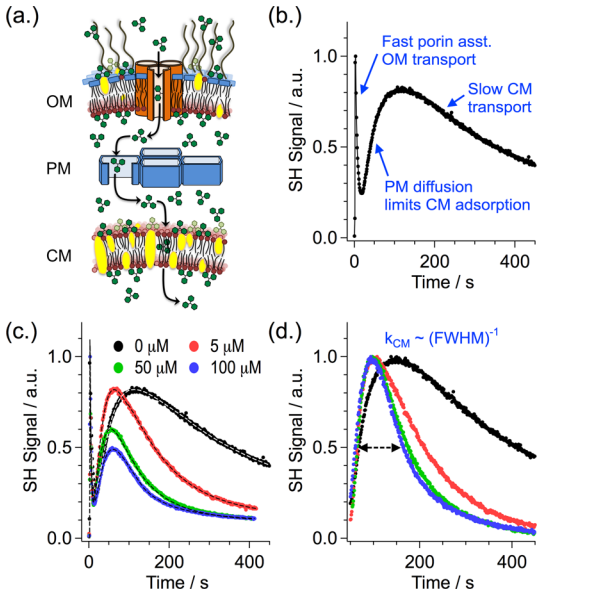

Figure 1. SHS characterizing molecular uptake in living cells. (a) Cartoon schematic of the general cellular ultrastructure of Gram-negative bacterial cells, consisting of an outer membrane (OM), a peptidoglycan mesh (PM), and a cytoplasmic membrane (CM). (b) Characteristic SHS response of malachite green (MG) uptake in *Escherichia coli*, exhibiting fast transport (narrow peak) across the OM and slow transport (broad peak) across the CM. (c) Perturbations to the MG SHS signal due to the co-presence of increasing concentrations of ATP, along with associated best fit results (dashed lines). (d) Cropped SHS signals, renormalized to the slow transport peak maxima, highlighting the ATP-induced contraction of the CM transport peak.

Received: June 2, 2015
Revised: June 19, 2015
Published: June 30, 2015

DOI: 10.1021/acs.biochem.5b00600
Biochemistry 2015, 54, 4427−4430

onto the outer surface of a membrane, a coherent SHS signal with an increasing magnitude can be detected. Over time, molecules traverse the membrane and begin adsorbing onto the opposing membrane surface. Significantly, molecules adsorbed on the opposing sides of a membrane exhibit opposite orientations. Subsequently, as SH fields generated from oppositely oriented molecules are necessarily out of phase, the overlapping fields destructively interfere, which results in an attenuation of the SHS signal. Overall, this sequential rise and decay of the signal is the characteristic SHS response to surface adsorption and membrane transport, with the decay rate of the corresponding SHS signal peak being proportional to the membrane crossing rate (see Figure 1b). In a qualitative sense, the membrane transport rate is inversely proportional to the full width at half-maximum (fwhm) of the SHS transport peak (i.e., narrow peaks suggest fast transport, and broad peaks suggest slow transport). This behavior was confirmed previously in experiments performed on liposomes[20−22] and living cells.[9−12]

In addition to its role as an intracellular energy source, adenosine triphosphate (ATP) is now well-recognized as a key extracellular signaling molecule.[23,24] Of significance, it has been established that the addition of extracellular adenosine triphosphate (ATPe) results in an increase in the passive permeability of membranes in a variety of cell types.[25−29] For instance, in mammalian cells, ATPe activates the so-called P_2 family of nucleotide receptors, which triggers the opening of pores and permits the free flow of ions across the membrane.[23,24] Conversely, the relative permeabilizing effect of ATPe, and associated mechanism of action, on bacterial membranes has yet to be characterized. This is particularly significant as ATPe, with its demonstrated effect on mammalian cell membrane permeability, could be viewed as potentially antimicrobial. Here we report a study establishing SHS as an effective time-resolved probe of chemically induced changes to membrane permeability by examining the effect of ATPe on molecular transport in living bacteria.

In this letter, we quantify the ATPe-induced permeabilizing effect on the membranes of the Gram-negative bacterium *Escherichia coli*. Figure 1a depicts the general membrane ultrastructure of Gram-negative bacteria, which is composed of two distinct anionically charged lipoprotein membranes: (1) a lipopolysaccharide-coated outer membrane (OM), which contains water-filled integral membrane protein channels (porins), and (2) an inner cytoplasmic membrane (CM), which acts as a protective barrier for the genetic material enclosed within the cytosol. The two membranes are separated by a thin peptidoglycan mesh (PM), which is covalently bound to the OM and acts as a diffusion barrier for transport across the periplasmic space. As discussed previously,[9,10,12] Figure 1b highlights the characteristic time-resolved SHS signal that reveals molecular uptake of the SHG-active cationic dye, malachite green (MG), across the dual membranes of living *E. coli*. Note that the porin channels in the OM allow rapid transport of MG, which gives rise to a narrow SHS peak with fast decay. Conversely, direct transport of the MG cation across the lipid bilayer of the inner CM is a comparatively slower process because of the diffusion limiting effect of the PM and the lack of passive transport channels in the CM. Here the SHS peak is significantly broader with a slower rise and decay. A nonlinear least-squares fit of the time-resolved SHS signal, based upon a previously described model of molecular uptake (see the Supporting Information for details),[9,10,12] allows direct quantification of the membrane-specific transport rates.

Panels c and d of Figure 1 show the effect of ATPe on the uptake kinetics of MG in living *E. coli*. Because of the high efficiency of transport across the OM porin channels, the addition of ATPe has no measurable effect on the kinetics of uptake of MG across the OM (Figure 1c, early time portion). However, there is a clear increase in the secondary rise of the SHS signal associated with adsorption of MG onto the CM. This suggests that the presence of ATPe allows a faster buildup of MG density on the CM outer surface. Conversely, the presence of increasing concentrations of ATPe has a remarkable influence on the transport of MG across the CM (Figure 1c,d). Note that laser irradiation (applied identically in all experiments) does not induce a measurable change in permeability. If this were not so, the measured SHS signals in panels c and d of Figure 1 would be indistinguishable.

Addition of ATPe results in two notable changes in the SHS peak relevant to transport across the CM: (1) a concentration-dependent narrowing of the fwhm, which is more apparent in the renormalized signal depicted in Figure 1d, and (2) an overall attenuation of the SHG signal. Both changes are indicative of an increase in the transport rate. As the kinetic model illustrates (see the Supporting Information for details), an increase in the signal decay rate causes a decrease in the overall magnitude of the detected signal.[9,10,12] Specifically, faster transport across the membrane simultaneously depletes the number of molecules on the outer leaflet of the membrane and increases the number of molecules adsorbed onto the inner leaflet of the membrane, resulting in a faster cancellation of the signal (i.e., due to destructive interference). Likewise, the faster transport rate is mimicked by a faster signal decay, which results in a narrowing of the measured transport peak.[9,10,12,20,22] Attenuation of the signal and the narrowness of the CM transport peak become more prominent because of the diffusion-limited transport of the molecules through the PM. Specifically, as opposed to the outer surface of the OM that is, on the time scale of our measurement, instantaneously coated following the addition of MG, diffusion across the PM significantly reduces the initial concentration of MG that reaches the CM, therefore slowing the rate of surface adsorption. Subsequently, as the permeability of the CM increases, molecular transport across the membrane begins to compete against accumulation of adsorbed molecules on the membrane surface.

A previously described comprehensive kinetic model, which has been shown to be effective in describing molecular adsorption at the membrane surfaces and transport into the cell, can be used for a nonlinear least-squares fit analysis of the time-resolved SHS data (see the Supporting Information for details). This model takes into account adsorption and desorption from available membrane surfaces; transport across the OM, PM, and CM; and time-dependent molecular concentrations within the extracellular space, the periplasmic space, and the cytosol. This model analysis allows experimental quantification of the ATP-induced changes in the permeability of the bacterial CM.[9,10,12] Best fit results for the time-dependent SHS signal are depicted in Figure 1c as dashed lines. The deduced variations in MG transport rates at the CM are plotted in Figure 2 and listed in Table 1. Significantly, we observe that the co-addition of equivalent concentrations of ATP and MG (i.e., 5 μM) effectively triples the MG transport rate at the CM. This enhancement is further increased to nearly an order of magnitude following the addition of 100 μM ATPe.

DOI: 10.1021/acs.biochem.5b00600
Biochemistry 2015, 54, 4427−4430

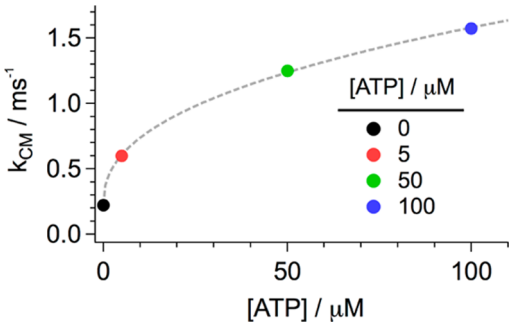

Figure 2. MG crossing rates at the CM in the presence of increasing concentrations of ATPe, deduced from fittings of the SHS results (Figure 1c). The gray dashed line represents a fitting of the rates to a simple power function as a guide for the eye.

Table 1. Measured CM Crossing Rates for 5.0 μM MG in *E. coli*, Deduced from Fittings of the SHS Results (Figure 1c)[a]

[ATP] (μM)	k_{CM} ($\times 10^{-4}$ s^{-1})
0	2.2 ± 0.11
5	6.0 ± 0.09
50	12.5 ± 0.11
100	15.7 ± 0.13

[a]Deduced rates obtained from experiments with three independent cell cultures and expressed as means ± the standard deviation.

To understand how ATPe may change the membrane permeability, a set of control experiments were performed with liposome membranes constructed from phospholipids isolated from *E. coli*. As shown in Figure 3, even high concentrations

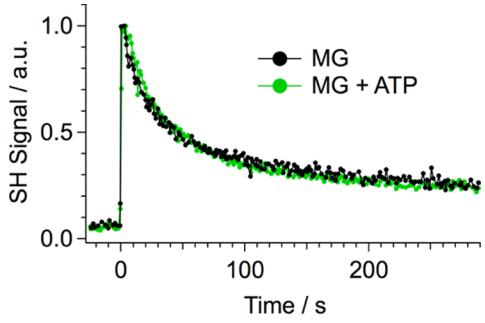

Figure 3. Invariant SHS for MG (5 μM) traversing a membrane of a unilamellar liposome (~122 ± 10 nm diameter), in the presence and absence of ATPe (100 μM).

(e.g., 100 μM) of ATPe are unable to change the permeability of the liposome membranes, which are ideal protein-free biomimetic surrogates of the CM. This observation strongly suggests that the permeabilization of the bacterial membrane is protein-mediated.

It is unclear, however, whether the protein-facilitated effect stems from the opening of an ATPe-activated passive transport channel, i.e., similar to that of the P_2 receptors in mammalian cells,[23,24] or from a change in the electrostatic interaction as a result of transport of ATP into the cytosol through nucleotide selective protein receptors. ATP is polyanionic; hence, its transport into the cytosol would result in a net reduction of the electrostatic potential of the cell's interior domain and aid in the transport of the cationic MG. Note that Eisenthal and co-workers have previously demonstrated the effect of the electrostatic potential change on the transport of hydrophobic ions across liposome membranes.[30] In that case, as the electrostatic potential increased following transport of cations into the liposome, the membrane crossing rate of the cations decreased because of the growing electrostatic repulsion. Conversely, a 4-fold increase in the rate of transport of MG in liposomes was observed following addition of the small-cation exporter, gramicidin A.[30] In our case, a reduction in the net electrostatic potential in the bacterial cytosol due to excess ATP would likely balance out the accumulating MG cationic charge during transport and increase the transport rate via electrostatic attraction.

Finally, even though our initial study focused solely on the membrane permeabilizing interaction of ATPe with bacterial cells, it should be noted that time-resolved SHS is generally applicable for quantifying permeability. In principle, provided a known SHG-active molecule (e.g., MG) is able to cross the membrane(s) in a cell of interest, either before or after administration of a permeabilizer, time-resolved SHS can be used to quantitatively characterize any permeability change. Given the inherent surface sensitivity, SHS is ideally suited for deducing the mechanism of action of antimicrobial peptides in living cells.

In summary, we observe that the addition of ATPe induces a significant enhancement of the permeability of the bacterial cytoplasmic membrane. Specifically, we used time-resolved SHS to directly quantify the enhanced permeability of the CM in living *E. coli*. Enhanced membrane permeability results in notable changes to the characteristic SHS transport peak. Specifically, a narrowing of the SHS peak and an overall attenuation of the total signal have been observed and are indicative of faster transport through the CM. Enhanced transport rates were quantified through a nonlinear least-squares fit analysis of the measured signals. Significantly, it was shown that the transport rate for MG at the CM can be increased by nearly an order of magnitude. Further, the complete absence of an ATPe-enhanced permeability in liposomes strongly suggests that the induced effect on bacterial membranes is protein-mediated, similar to that in mammalian cells. Nevertheless, the exact mechanism is still to be determined. Finally, while we have focused specifically on bacteria and ATPe, the described methodology is fully amenable for the real-time quantitative characterization of membrane permeability in any combination of cells and membrane permeabilizers.

■ ASSOCIATED CONTENT

Supporting Information

Full experimental methods and a kinetic model of molecular uptake. The Supporting Information is available free of charge on the ACS Publications website at DOI: 10.1021/acs.biochem.5b00600.

■ AUTHOR INFORMATION

Corresponding Author

*E-mail: michael.wilhelm@temple.edu. Phone: (215) 204-2836.

Author Contributions

M.J.W. and H.-L.D. conceived and designed the experiments. M.J.W. and M.S.G. performed the experiments. M.J.W. analyzed the data. M.J.W., M.S.G., and H.-L.D. interpreted the results. M.J.W. and H.-L.D. wrote the manuscript.

DOI: 10.1021/acs.biochem.5b00600
Biochemistry 2015, 54, 4427−4430

Funding

This work was supported by the National Science Foundation (Grant CHE-1465096).

Notes

The authors declare no competing financial interest.

■ ACKNOWLEDGMENTS

We are grateful to Allen Nicholson (Temple University) for assistance with cell culturing techniques.

■ REFERENCES

(1) Centers for Disease Control and Prevention (2013) Antibiotic Resistance Threats in the United States, 2013, Centers for Disease Control and Prevention, Atlanta.

(2) Ling, L. L., Schneider, T., Peoples, A. J., Spoering, A. L., Engels, I., Conlon, B. P., Mueller, A., Hughes, D. E., Epstein, S., Jones, M., Lazarides, L., Steadman, V. a, Cohen, D. R., Felix, C. R., Fetterman, K. A., Millett, W. P., Nitti, A. G., Zullo, A. M., Chen, C., and Lewis, K. (2015) A new antibiotic kills pathogens without detectable resistance. *Nature 517*, 455−459.

(3) Brogden, K. A. (2005) Antimicrobial peptides: Pore formers or metabolic inhibitors in bacteria? *Nat. Rev. Microbiol. 3*, 238−250.

(4) Melo, M. N., Ferre, R., and Castanho, M. A. R. B. (2009) Antimicrobial peptides: Linking partition, activity and high membrane-bound concentrations. *Nat. Rev. Microbiol. 7*, 245−250.

(5) Hancock, R. E. (2001) Cationic peptides: Effectors in innate immunity and novel antimicrobials. *Lancet Infect. Dis. 1*, 156−164.

(6) Henriques, S. T., Melo, M. N., and Castanho, M. a R. B. (2006) Cell-penetrating peptides and antimicrobial peptides: How different are they? *Biochem. J. 399*, 1−7.

(7) Mensa, B., Kim, Y. H., Choi, S., Scott, R., Caputo, G. a., and DeGrado, W. F. (2011) Antibacterial mechanism of action of arylamide foldamers. *Antimicrob. Agents Chemother. 55*, 5043−5053.

(8) Mensa, B., Howell, G. L., Scott, R., and DeGrado, W. F. (2014) Comparative mechanistic studies of brilacidin, daptomycin, and the antimicrobial peptide LL16. *Antimicrob. Agents Chemother. 58*, 5136−5145.

(9) Zeng, J., Eckenrode, H. M., Dounce, S. M., and Dai, H.-L. (2013) Time-resolved molecular transport across living cell membranes. *Biophys. J. 104*, 139−145.

(10) Wilhelm, M. J., Sheffield, J. B., Gonella, G., Wu, Y., Spahr, C., Zeng, J., Xu, B., and Dai, H.-L. (2014) Real-time molecular uptake and membrane-specific transport in living cells by optical microscopy and nonlinear light scattering. *Chem. Phys. Lett. 605−606*, 158−163.

(11) Zeng, J., Eckenrode, H. M., Dai, H.-L., and Wilhelm, M. J. (2015) Adsorption and transport of charged vs. neutral hydrophobic molecules at the membrane of murine erythroleukemia (MEL) cells. *Colloids Surf., B 127*, 122−129.

(12) Wilhelm, M. J., Sheffield, J. B., Sharifian Gh, M., Wu, Y., Spahr, C., Gonella, G., Xu, B., and Dai, H.-L. (2015) Gram's stain does not cross the bacterial cytoplasmic membrane. *ACS Chem. Biol. 10*, 1711−1717, DOI: 10.1021/acschembio.5b00042.

(13) Shen, Y. R. (1989) Surface properties probed by second-harmonic and sum-frequency generation. *Nature 337*, 519−525.

(14) Eckenrode, H. M., and Dai, H.-L. (2004) Nonlinear optical probe of biopolymer adsorption on colloidal particle surface: Poly-L-lysine on polystyrene sulfate microspheres. *Langmuir 20*, 9202−9209.

(15) Fu, L., Xiao, D., Wang, Z., Batista, V. S., and Yan, E. C. Y. (2013) Chiral sum frequency generation for in situ probing proton exchange in antiparallel beta-sheets at interfaces. *J. Am. Chem. Soc. 135*, 3592−3598.

(16) Wang, J., Chen, X., Clarke, M. L., and Chen, Z. (2005) Detection of chiral sum frequency generation vibrational spectra of proteins and peptides at interfaces in situ. *Proc. Natl. Acad. Sci. U. S. A. 102*, 4978−4983.

(17) Wang, J., Paszti, Z., Even, M. a., and Chen, Z. (2002) Measuring polymer surface ordering differences in air and water by sum frequency generation vibrational spectroscopy. *J. Am. Chem. Soc. 124*, 7016−7023.

(18) Yan, E. C. Y., Fu, L., Wang, Z., and Liu, W. (2014) Biological macromolecules at interfaces probed by chiral vibrational sum frequency generation spectroscopy. *Chem. Rev. 114*, 8471−8498.

(19) Gonella, G., and Dai, H.-L. (2011) Determination of adsorption geometry on spherical particles from nonlinear Mie theory analysis of surface second harmonic generation. *Phys. Rev. B: Condens. Matter Mater. Phys. 84*, 121402.

(20) Srivastava, A., and Eisenthal, K. B. (1998) Kinetics of molecular transport across a liposome bilayer. *Chem. Phys. Lett. 292*, 345−351.

(21) Yamaguchi, A., Nakano, M., Nochi, K., Yamashita, T., Morita, K., and Teramae, N. (2006) Longitudinal diffusion behavior of hemicyanine dyes across phospholipid vesicle membranes as studied by second-harmonic generation and fluorescence spectroscopies. *Anal. Bioanal. Chem. 386*, 627−632.

(22) Yan, E. C. Y., and Eisenthal, K. B. (2000) Effect of cholesterol on molecular transport of organic cations across liposome bilayers probed by second harmonic generation. *Biophys. J. 79*, 898−903.

(23) Gordon, J. L. (1986) Extracellular ATP: Effects, sources and fate. *Biochem. J. 233*, 309−319.

(24) Khakh, B. S., and North, R. A. (2006) P2X receptors as cell-surface ATP sensors in health and disease. *Nature 442*, 527−532.

(25) Trams, E. G. (1974) Evidence for ATP action on the cell surface. *Nature 252*, 480−482.

(26) Dicker, P., Heppel, L. A., and Rozengurt, E. (1980) Control of membrane permeability by external and internal ATP in 3T6 cells grown in serum-free medium. *Proc. Natl. Acad. Sci. U. S. A. 77*, 2103−2107.

(27) Bennett, J. P., Cockcroft, S., and Gomperts, B. D. (1981) Rat mast cells permeabilized with ATP secrete histamine in response to calcium ions buffered in the micromolar range. *J. Physiol. 317*, 335−345.

(28) Chahwala, S. B., and Catley, L. C. (1984) Extracellular ATP induces ion fluxes and inhibits growth of Friend erythroleukemia cells. *J. Biol. Chem. 259*, 13717−13722.

(29) Weisman, G. a, De, B. K., Friedberg, I., Pritchard, R. S., and Heppel, L. a. (1984) Cellular responses to external ATP which precede an increase in nucleotide permeability in transformed cells. *J. Cell. Physiol. 119*, 211−219.

(30) Liu, J., Subir, M., Nguyen, K., and Eisenthal, K. B. (2008) Second harmonic studies of ions crossing liposome membranes in real time. *J. Phys. Chem. B 112*, 15263−15266.

DOI: 10.1021/acs.biochem.5b00600
Biochemistry 2015, 54, 4427−4430